

Better latent heat and specific heat of stearic acid with magnetite/graphene nanocomposite addition for thermal storage application

R Andiar^{1,2}, M K Nuryadin^{1,2}, A Taufik^{1,2} and R Saleh^{1,2}

¹Department of Physics, Faculty of Mathematics and Natural Sciences Universitas Indonesia, Kampus UI Depok, Depok 16424, Indonesia

²Integrated Laboratory of Energy and Environment, Faculty of Mathematics and Natural Sciences Universitas Indonesia, Kampus UI Depok, Depok 16424, Indonesia

Corresponding author's e-mail: rosari.saleh@gmail.com

Abstract. In our previous study, the addition of Magnetite (Fe_3O_4) into Stearic acid (Sa) as an organic phase change material (PCM) shows an enhancement in the latent heat for thermal energy storage applications. The latent heat of the PCM can also be increased by adding graphene material. Therefore, in this research, the thermal properties of Sa have been studied by the sonication method for several different concentrations of Fe_3O_4 /Graphene nanocomposite additions. The structural properties of all of the samples were observed by X-Ray diffraction (XRD). Melting-solidifying behavior and specific heat value were measured by differential scanning calorimetry (DSC). The thermal degradation process of all samples was investigated by thermogravimetric analysis (TGA). Based on the DSC results, the presence of Fe_3O_4 /Graphene in the Sa enhances the latent heat up to 20%. The specific heat value of the mixture was also found to be increased as the concentration of Fe_3O_4 /Graphene to Sa increased. The TGA results show a lowered thermal degradation process of the Sa by the addition of the Fe_3O_4 /Graphene which indicates a higher thermal stability of the mixture. In conclusion, the results demonstrate that the addition of Fe_3O_4 /Graphene to Sa improves both the sensible heat and the latent heat of the mixture which are very important for thermal energy storage applications

Keywords: Phase change materials, Fe_3O_4 , graphene, latent heat

1. Introduction

Thermal energy storage (TES) based on phase change material (PCM) utilization has resulted an advancement in thermal energy applications [1-2]. The use of PCM for TES applications also has a great potential in many fields such as solar cell efficiency, heating and cooling building conservation systems, and thermal regulating textile materials [3-5]. From the various types of PCM, Stearic acid (Sa) is considered to be the most recommended organic PCM for TES applications due to its advantageous features, such as: non-toxic, non-corrosive, and applicable phase change temperature [6-7]. However, the using of stearic acid as PCMs materials still has a limitation due to low thermal conductivity of stearic acid. many researchers are trying to find ways to enhance the ability of PCMs in order to store and release heat so it can be used in large scale applications [8]. One of the most promising methods for enhancing the ability of a PCM to store and release heat is by adding nanoparticles to the PCM [9].



In our previous study, the addition of the magnetite metal oxide material (Fe_3O_4) into the Sa resulted an enhancement in the latent heat value of the Sa [10]. Those results are supported by another study in which Fe_3O_4 nanoparticles were added to improve the ability of the organic PCM [11]. Moreover, the addition of carbon-based nanomaterials into the PCM also show an increment in the latent heat value of the PCM [12]. Based on above explanations, combining Fe_3O_4 and graphene materials is become a promising method for enhance the PCM performance. Therefore, in this study, Fe_3O_4 /Graphene nanocomposite was synthesized using the hydrothermal method and then mixed with Sa in the various concentrations of 0.3, 0.5, 0.8, 1, and 5% wt (weight transfer) to form a Sa/ Fe_3O_4 /Graphene mixture. Thermal investigation was then carried out in order to observe the thermal properties of the samples to determine their effectiveness for use in TES applications.

2. Experimental setup

In this study, Stearic acid ($\text{C}_{17}\text{H}_{35}\text{CO}_2\text{H}$) was used as a phase change material. Iron (II) sulfate heptahydrate ($\text{FeSO}_4 \cdot 7\text{H}_2\text{O}$), sodium hydroxide (NaOH), and ethylene glycol were used to synthesize Fe_3O_4 nanoparticles. The synthesis process followed the same method as our previous study [13]. All of the reagents were purchased from Merck and used without further purification. The synthesized Fe_3O_4 was then combined with Graphene (Angstrom Materials) to form a Fe_3O_4 /Graphene nanocomposite using the hydrothermal method with 5 wt.% Graphene added to the Fe_3O_4 . In brief, the synthesis process of the Fe_3O_4 /Graphene nanocomposite was started by sonicating Graphene with distilled water for 2 hours. The resulting solution was then mixed with Fe_3O_4 nanoparticles and then stirred with a magnetic stirrer. The mixture that formed was then heated at 70°C for 3 hours. The Fe_3O_4 /Graphene nanocomposite which formed was then centrifuged and heated at 70°C for 12 hours in vacuum conditions. The combination of the Stearic acid (Sa) with the Fe_3O_4 /Graphene nanocomposite was performed by dispersing the desired amount of the Fe_3O_4 /Graphene (0.3, 0.5, 0.8, 1, and 5% wt) into the Sa in an ultrasonic bath for 2 hours.

The structural properties of the Fe_3O_4 /Graphene nanocomposite and Sa/ Fe_3O_4 /Graphene mixtures were characterized by X-Ray diffraction (XRD). Thermogravimetric analysis (TGA) was also performed in order to prove the presence of Graphene in the Fe_3O_4 /Graphene nanocomposite. The thermal degradation process of the samples was also observed through TGA while the differential thermogravimetric analysis (DTGA) was calculated based on the TGA data. For the thermal properties of the Sa/ Fe_3O_4 /Graphene samples, differential scanning calorimetry (DSC) was used in order to observe the phase transformation process, the latent heat value, and the specific heat value (C_p).

3. Results and discussion

The presence of Graphene in the Fe_3O_4 /Graphene nanocomposite was proved by the TGA results as shown in figure 1a. The TGA measurements were investigated in order to determine the thermal degradation process of the nanocomposite. As can be seen in figure 1a, the degradation process was started at 400°C which indicates the combustion effect from the Graphene [14]. Moreover, the percentage loss residue at the end of measurement at 1000°C shows the composition of Graphene in the Fe_3O_4 /Graphene nanocomposite which is about 5% wt. This result confirms the presence of Graphene in the Fe_3O_4 /Graphene nanocomposite.

The XRD results of the Fe_3O_4 /Graphene nanocomposite, along with the Sa and Sa/ Fe_3O_4 /Graphene 5% wt, are shown in figure 1b. Based on the XRD spectrum of Fe_3O_4 /Graphene, there are peaks that can be seen at the $2\theta \approx 30.2^\circ$, 35.5° , 53.4° , and 57.0° which represent the (220), (311), (511), and (440) planes of the inverse cubic spinel structure of Fe_3O_4 . There is no sign of the Graphene peak pattern in the Fe_3O_4 /Graphene XRD measurement which is due to Graphene's amorphous properties [15]. For the Sa spectrum shown in figure 1b, there are two readily indexed peaks at $2\theta \approx 21.3^\circ$ and 24.7° which show the regular crystallization pattern of the Sa. The XRD measurement of the Sa/ Fe_3O_4 /Graphene shows the combination between the crystallinity peak patterns of Fe_3O_4 /Graphene and Sa which confirms the presence of the desired Fe_3O_4 /Graphene crystallinity in the Sa. The melting and solidifying

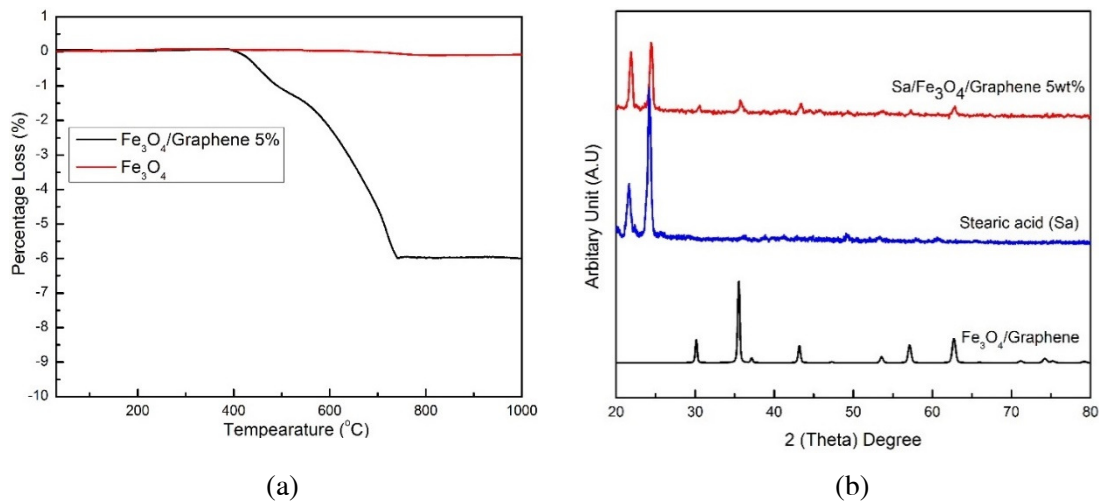


Figure 1. (a) TGA results for Fe_3O_4 nanoparticle and $\text{Fe}_3\text{O}_4/\text{Graphene}$ nanocomposite, and (b) XRD spectrum for $\text{Fe}_3\text{O}_4/\text{Graphene}$, Sa and $\text{Sa}/\text{Fe}_3\text{O}_4/\text{Graphene}$ 5 wt.%.

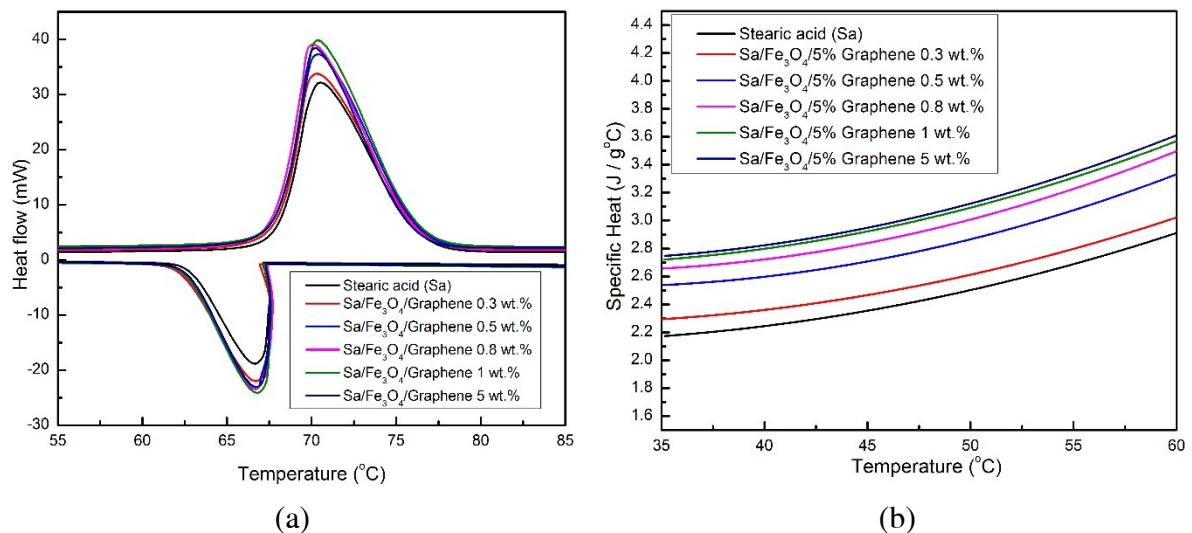


Figure 2. (a) DSC curve of $\text{Sa}/\text{Fe}_3\text{O}_4/\text{Graphene}$ in all variation, and (b) fitting curve of $\text{Sa}/\text{Fe}_3\text{O}_4/\text{Graphene}$ specific heat in all variation.

process of the $\text{Sa}/\text{Fe}_3\text{O}_4/\text{Graphene}$ mixtures was measured and analyzed through DSC. The phase change process of the PCM indicates the main characteristic of the PCM as an application for latent heat thermal storage (LHTS) [16]. The resulting curve of DSC measurements is shown in figure 2a. Based on the results, it can be seen that all of the samples performed the one-step process of endothermic and exothermic under melting and solidifying process. Qualitatively, the total area under the curve shows how much heat is involved in the phase change process. As can be seen in figure 2a, the area under the DSC curve of the $\text{Sa}/\text{Fe}_3\text{O}_4/\text{Graphene}$ shows a larger curve than the Sa alone. This signifies the enhancement of the heat involved during the store and release process in the phase change process [11]. The resulting DSC curves shown in figure 2a also provide information about the melting point temperatures and solidifying point temperatures alongside the latent heat values which are calculated through the integration of the area under the DSC curve. All of the data from the DSC curve are tabulated in table 1. Based on the data, it can be concluded that the addition of the $\text{Fe}_3\text{O}_4/\text{Graphene}$

nanocomposite to the Sa did not have any favorable effect on the melting and solidifying temperature behavior of the Sa. However, the latent heat value calculation for the Sa was found to be enhanced by the presence of Fe₃O₄/Graphene. The latent heat value of the Sa was found to increase as the concentration of Fe₃O₄/Graphene increased. The maximum enhancement was found at the 1% wt concentration of the Fe₃O₄/Graphene to Sa ratio. This result shows that the addition of Fe₃O₄/Graphene to Sa enhances the capability of the Sa to store and release heat. The enhancement of the Sa's latent heat value due to the presence of Fe₃O₄/Graphene can be explained by the intermolecular interaction between the Sa and the Fe₃O₄/Graphene [12].

The specific heat (C_p) calculations were also analyzed using the corresponding DSC curves in order to observe the sensible heat ability for the sensible heat storage application [17]. The specific heat calculations from 35°C to 65°C are shown in figure 2b. Based on the results, it can be determined that as the concentration of the Fe₃O₄/Graphene in the Sa increased, the specific heat value of the Sa/Fe₃O₄/Graphene mixture also increased. The enhancement of the specific heat can also be seen from the average heat value which is shown in table 2. Based on the average value, the maximum enhancement of specific heat was found at the concentration of 5% wt of Fe₃O₄/Graphene.

The thermal degradation process of the Sa/Fe₃O₄/Graphene in all variations was observed through TGA. The results are shown in figure 3a. The onset and percentage loss data based on the corresponding TGA curves are tabulated in table 2. Based on those results, it can be observed that the

Table 1. Solid-liquid, liquid-solid temperature data and latent heat value for melting and solidifying process of Sa/Fe₃O₄/Graphene in all variation.

Sample	Solid-liquid	liquid-solid	Melting	solidifying
	T _{peak}	T _{onset}	ΔH _m (J/g)	ΔH _s (J/g)
Stearic acid (Sa)	70.5	67	177.6	174.1
Sa/Fe ₃ O ₄ /Graphene 0.3%	70.2	67.3	199.7	196.3
Sa/Fe ₃ O ₄ /Graphene 0.5%	70.4	67.4	210.3	206.8
Sa/Fe ₃ O ₄ /Graphene 0.8%	70.1	67.2	214.5	212
Sa/Fe ₃ O ₄ /Graphene 1%	70.2	67.3	216.6	213.2
Sa/Fe ₃ O ₄ /Graphene 5%	70.2	67.3	199	194.5

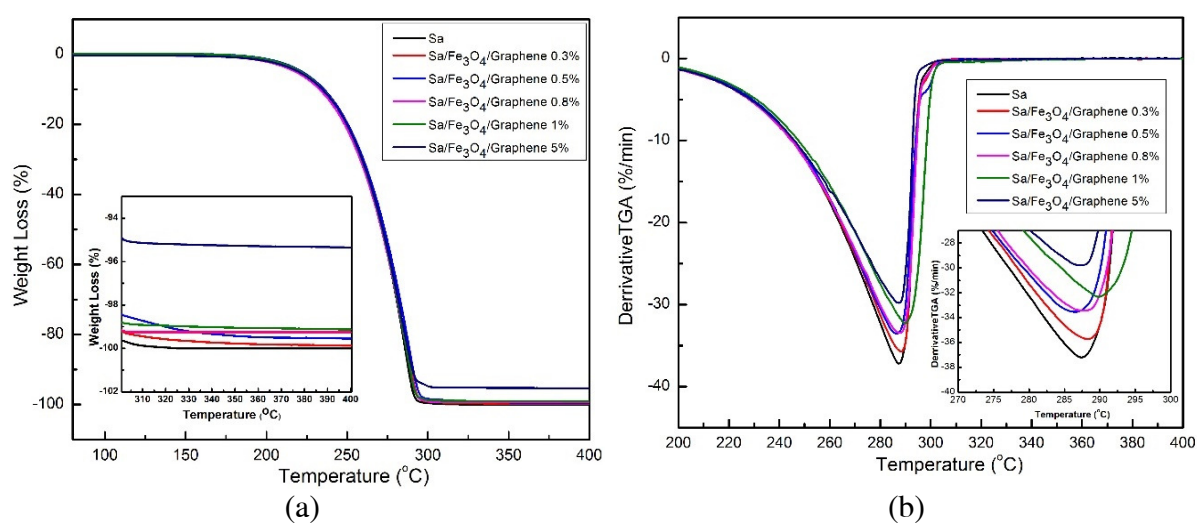


Figure 3. TGA curve (a) and DTGA curve (b) for the Sa/Fe₃O₄/Graphene in all variation.

Table 2. Average Specific heat (C_p) value calculation of Sa/Fe₃O₄/Graphene in all variation.

Samples	Average C_p (J/g°C)	Onset (°C)	Percentage weight lost (%)
Stearic acid (Sa)	2.48	251.6	100
Sa/Fe ₃ O ₄ /Graphene 0.3%	2.59	254	99.6
Sa/Fe ₃ O ₄ /Graphene 0.5%	2.84	253.3	99.59
Sa/Fe ₃ O ₄ /Graphene 0.8%	2.97	253.6	99.19
Sa/Fe ₃ O ₄ /Graphene 1%	3.03	255.5	99.08
Sa/Fe ₃ O ₄ /Graphene 5%	3.06	254.1	94.91

Sa/Fe₃O₄/Graphene mixture in all variations has a strong thermal stability up to 200 °C. The degradation process was found to suffer from gradual weight loss at 250°C which was due to the evaporation process of the Sa. Furthermore, the percentage loss data shows that the Fe₃O₄/Graphene was in the appropriate composition of variation.

Using the TGA results, differential thermogravimetric analysis was performed to calculate how fast the degradation process occurred due to temperature for each sample. The DTGA results are shown in figure 3b. The lowest peak indicates the faster degradation process of the Sa. As can be seen in the DTGA curve, the addition of Fe₃O₄/Graphene into the Sa can slow the degradation process. Some research has previously stated that the slower degradation process may result in an incremental increase in the thermal stability of the PCM [18].

4. Conclusions

Fe₃O₄/Graphene has been successfully synthesized through the sol-gel method and used as an additive material into Sa. The DSC results show that the latent heat value of the Sa increases due to the addition of the Fe₃O₄/Graphene with the maximum enhancement at 1% wt of Fe₃O₄/Graphene. Furthermore, the increments can be found in the specific heat results with the maximum enhancement at 5% wt of Fe₃O₄/Graphene. The enhancement of both latent heat and specific heat also shows that the Sa/Fe₃O₄/Graphene mixture is suitable for latent heat and sensible heat storage. Moreover, the thermal stability of the Sa was found to be enhanced due to the presence of the Fe₃O₄/Graphene as seen by the slower degradation process.

References

- [1] Regin A F, Solnaki S C and Saini J S 2008 *Renew. Sustainable Energy Rev.* **12** 2438-58
- [2] Sharma A, Tyagi V V, Chen C R and Buddhi D 2009 *Renew. Sustainable Energy Rev.* **13** 318-45
- [3] Tyagi V V and Buddhi D 2007 *Renew. Sustainable Energy Rev.* **11** 1146-66
- [4] Khodadadi J M, Fan L and Babaei H 2013 *Renew. Sustainable Energy Rev.* **24** 418-44
- [5] Mondal S 2008 *Appl. Therm. Eng.* **28** 1536-50
- [6] Zalba B, Marin J M, Cabeza L F and Mehling H 2003 *Appl. Therm. Eng.* **23** 251-83
- [7] Cao L, Tang Y and Fang G 2015 *Energy* **80** 98-103
- [8] Feldman D, Shapiro M M, Banu D and Fuks C J 1989 *Sol. Energ. Mat. Sol.* **18** 201-16
- [9] Kibria M A, Anisur M R, Mahfuz M H, Saidur R and Metselaar H S C 2015 *Energy Convers. Manage.* **95** 69-89
- [10] Andiarto R, Nuryadin M K and Saleh R 2016 *J. Phys. Conf. Ser.* **710** 012020
- [11] Sahan N and Paksoy H O 2014 *Sol. Energ. Mat. Sol.* **126** 56-61
- [12] Shaikh S, Lafdi K and Hallinan K 2008 *J. Appl. Phys.* **103** 094302
- [13] Arifin S A, Jalaludin S and Saleh R 2015 *Adv. Mat. Res.* **1123** 264-9
- [14] Loryuenyong V, Totepvimarn K, Eimburanapravat P, Boonchompoo W and Buasri A 2013 *Adv. Mater. Sci. Eng.* **2013** 923403
- [15] Ferrari A C 2007 *Solid State Commun.* **143** 47-57

- [16] Sharma R K, Ganesan P, Tyagi V V, Metselaar H S C and Sandaran S C 2016 *Appl. Therm. Eng.* **99** 1254-62
- [17] Chieruzzi M, Cerritelli G F, Miliozzi A and Kenny J M 2013 *Nanoscale Res. Lett.* **8** 448
- [18] Tahan S, Mehrali M, Mehrali M, Meurah T, Mahlia I, Simon H and Metselaar C 2013 *Energy* **61** 664-72